IJISET - International Journal of Innovative Science, Engineering & Technology, Vol. 2 Issue 4, April 2015.
www.ijiset.com
ISSN 2348 – 7968

Analysis of Transonic Flow over an Airfoil NACA0012 using CFD

Novel Kumar Sahu[1], Mr.Shadab Imam[2],

[1]Department of Mechanical Engineering,
Christen College of Engineering & Technology, Bhilai, CG,
[2]Assistant Professor in Mechanical Department,
Christen College of Engineering & Technology, Bhilai, CG,

Abstract— Generally airplanes follow specific flight profiles consists of take-off, climb, cruise, descend and landing. These flight profiles fundamentally change the free-stream conditions in which the aircrafts operate. In the transonic speed the presences of nonlinearities adversely affects the aerodynamic performance on an Airfoil.
The present work deals with the comparative analysis of variation in Angle of attack and Mach number over NACA0012 Airfoil. The Transonic Compressible flow simulation has been carried using Spalart-Allmaras and k-ω turbulence model and PRESTO solution technique has been applied to govern Euler and Navier-Stokes continuity principle.
with the help of Aerodynamic Characteristic of airfoil such as Static and Dynamic pressure, Skin friction coefficient, wall shear stress, turbulence intensity in transonic regime the performance parameters of airfoil such as Angle of Attack, Lift Coefficient, Drag Coefficient has been analyzed and predicted with the help of Finite element volume tool ANSYS- Fluent. The FEV results are validated with well published results in literature and furthermore with experimentation. The FEV and experimental results show good agreement. As per which graph and figure are generated and discussed in the Paper.
Keywords*: Airfoil, NACA0012, Angle of Attack, Mach no.*

I. INTRODUCTION

Transonic flows signify to many complex phenomena, contact discontinuities, such as creation of shock, buffet onset and shock-boundary-layer interaction. Since these flows are robustly time-dependent Such flows are robustly time-dependent and cannot be fully implicit without reference to viscous Character of the fluid, as viscous terms are significant in their interaction with the convective process .
In real viscous flows, a change in flow field occurs in non-monotonic trend and leads to surface instability, even in the absence of unsteady boundary conditions. Therefore, transonic flows must be illustrated by the time dependent, compressible Navier–Stokes equations. Numerical methods for solving Navier–Stokes equations must be capable of predicting all the above flow characteristics accurately. Turbulent shock/boundary-layer interaction adjacent to an airfoil's surface has a intensely effect on the aerodynamic performance of a transonic aircraft due to the rapid thickening of boundary layers induced by the shock.
When the shock is adequately strong to provoke boundary-layer separation, a `k- shock' structure originates close to the separation point. This extensively affects the resulting drags and lift coefficients. The concurrent presence of High pressure gradient, shear, and recirculation related curvature close to a solid surface leads to a complex, highly anisotropic turbulence of structure. Extensive occurrence with such conditions in incompressible flows recommends that advanced modeling practices, based on second-moment closure, are often essential for a satisfactory prediction of recirculation.

II. LITERATURE REVIEW

Airfoil [2] several case studies are performed along with considering moving shock wave in order to predict the aero-elastic behavior of variable-sweep wing and the obtained result are compared with experimental result. Moreover the effect aero elastic damping is studied.
Kaynak and flores 1989 applied Euler/Navier-Stokes zonal approach for analyzing Transonic flow around the low aspect ratio wing in a wind tunnel. In their approach, global grid which had coarse grid is suitably clustered for viscous resolution [3]
Mahajan et. al 1991 solve Navier stokes equation by applying Lanczos approach for computing the Eigen vaules and Eigen vector for air foils. [4] The method of solving contains a combination of lopsided iteration and block tri-diagonal matrices.
In 1996 Yang and lee perform transonic aero-elastic analyses for a flap of airfoil. The aerodynamic calculation is solved by finite volume scheme. Runge-Kutta time stepping method has been used for determining unsteady aerodynamic forces and the time responses of aero-elastic system. [5]
Iollo and Salas 1999 use least square method for

ISSN 2348 – 7968

evaluating pressure distributions over a surface in transonic flight regimes.[6] The flow model governs Euler equation. And the pseudo time method is adopted for the Fast convergence to achieve the optimal solution.

Lien and Kalitzin 2001 exercise k–ε–v′2 model of Durbin is applied to the transonic flows over the Delery bump and the RAE 2822 airfoil considering the shock wave effect on both cases. [7] In computational domain elliptic relaxation equation of the model is employed for obtaining result for both supersonic and subsonic regimes. The accuracy of results has compared with experimental data and is within acceptable limit.

Fort et.al 2003 presents a numerical method for solving transonic flows over 2D airfoils and 3D wings. Lax-Wendroff scheme and multistage Runge-Kutta finite volume method adopted to solve 2D transonic turbulent flows with k-ω turbulent model over RAE 2822 airfoil and also 3D transonic in-viscid flows over a wing or wing-body combination.[8]

yongsheng et. al 2003 examines the effect of the flap movement on the separation location and vortex dynamics by comparing computational and experimental results simultaneously at high Reynolds number. [9]

In 2003 transonic aerodynamic shape optimization Wang proposed a Hierarchical evolutionary algorithms based genetic algorithm and Nash strategy of game theory. The proposed optimization scheme is applied over NACA0012 airfoil and found that airfoil has been optimized in maximizing the lift coefficient under a specified transonic flow condition.[10]

Jose et. al 2006 evaluate the feasibility of controlling the shock/boundary layer via numerical approach and found that proper selection of amplitude-frequency, momentum and location of the synthetic jet on airfoil surface, desired modulation in drag, lift and pitching moment coefficients can be attained for a given free-stream.[11]

Cinnella 2008 High-performance airfoils for transonic viscous flows of dense gases are constructed using an efficient high-order accurate flow solver coupled with a multi-objective genetic algorithm.[12]

Wollblad et. al 2010 Large eddy simulations were made of transonic flow over a two-dimensional bump where shock wave/turbulent boundary layer interaction takes place. Different flow conditions were investigated to find conditions for large scale shock movement. [13]

Remi et. al 2011 develop reduced-order model for predicting unsteady behavior of airfoil at transonic flows at moderate reynold number. The equation of motion is solved by using Galerkin projection and Hadamard formulation.[14]

Kuzmin 2012 presents a review of transonic flow problems that admit multiple numerical solutions at given stationary boundary conditions. Consider turbulent and inviscid flow over past symmetric and asymmetric airfoils. [16]

Tapa et. al 2013 develop highly time accurate Navier stokes solver for transonic flow for NACA0012. The solver uses optimized upwind compact schemes and explicit Runge kutta method to solve the N-S equation. It is found that the develop scheme is robust and shows good accuracy with experimental result and helps in exploring shock formation, drag divergence and buffet onset of flow over airfoils.[17]

Joachim et. al 2014 employ particle image velocimetry for analyzing the influence of leading edge modification on the time-averaged and instantaneous flow around a fan airfoil. [18].

Mukesh et. al 2014 develop a MATLAB program to implement PARSEC Panel Technique, and Genetic Algorithm. The program is tested for standard NACA 2411 airfoil and optimized to optimize to advances its coefficient of lift. Panel method is adopted to determine Pressure distribution and co-efficient of lift for airfoil geometries. [19]

Yang et. al 2015 develop a novel global optimization algorithm named as particle swarm optimization combined with particle generator (PSO–PG).through this algorithm the calculation accuracy has not only been improved but also optimize the system efficiency. The aerodynamic characteristics are well compared with the experimental result and shows good agreement. [20].

III. MATHEMATICAL MODEL

The equations governing this problem are those of Navier-Stokes along with the energy equation. The Navier-Stokes equations are applied to incompressible flows and Newtonian fluids, including the continuity equation and the equations of conservation of momentum on the x and y.

According to equations

$$\frac{\partial u_2}{\partial t} + u_1 \frac{\partial u_1}{\partial x_1} + u_2 \frac{\partial u_1}{\partial x_2} =$$

$$-\frac{1}{\rho}\frac{\partial \rho}{\partial x_2} + \nu\left(\frac{\partial^2 u_1}{\partial x_1^2} + \frac{\partial^2 u_1}{\partial x_2^2}\right) + g\,\beta\,(T - T\infty)$$

$$\frac{\partial u_1^*}{\partial x_1^*} + \frac{\partial u_2^*}{\partial x_2^*} = 0$$

X_1 momentum equation

ISSN 2348 – 7968

$$\frac{\partial u_1^*}{\partial t^*} + u_1^* \frac{\partial u_1^*}{\partial x_1^*} + u_2^* \frac{\partial u_1^*}{\partial x_2^*} = -\frac{\partial p^*}{\partial x_1^*} + \Pr\left(\frac{\partial u_1^*}{\partial x_1^*} + \frac{\partial u_1^*}{\partial x_2^*}\right)$$

X_2 momentum equation

$$\frac{\partial u_2^*}{\partial t^*} + u_1^* \frac{\partial u_2^*}{\partial x_1^*} + u_2^* \frac{\partial u_1^*}{\partial x_2^*} = -\frac{\partial p^*}{\partial x_2^*} + \Pr\left(\frac{\partial u_2^*}{\partial x_1^*} + \frac{\partial u_2^*}{\partial x_2^*}\right)$$

$$+Gr\,\Pr^2 T^*$$

Energy equation

$$\frac{\partial T^*}{\partial t^*} + u_1^* \frac{\partial T^*}{\partial x_1^*} + u_2^* \frac{\partial T^*}{\partial x_2^*} = \left(\frac{\partial^2 T^*}{\partial x_1^{*2}} + \frac{\partial^2 T^*}{\partial x_2^{*2}}\right)$$

(16)

IV. METHODOLOGY

The ANSYS 14.5 finite element program was used for analyzing NACA0012 Airfoil. For this purpose, the key points were first created and then line and spline segments were formed. The lines were combined to create an area. Finally, this area was extruded a We modeled the Airfoil. A 20-node three-dimensional structural solid element was selected to model the Airfoil. The Airfoil was discretized into 19325 elements with 10075 nodes. The Airfoil surface boundary conditions can also be (provided in mesh section through naming the portion of modeled Airfoil i.e Wall-top, Wall bottom, interior, pressure-far-field.

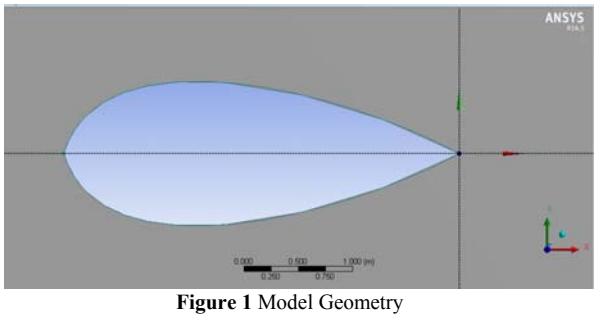

Figure 1 Model Geometry

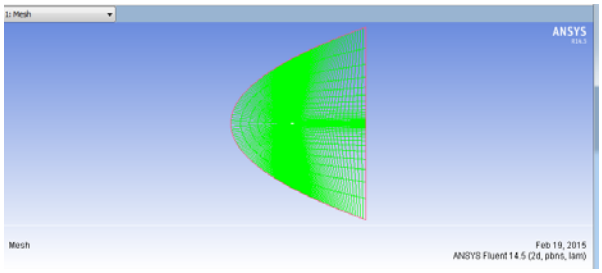

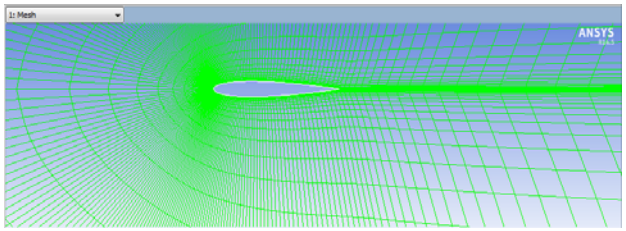

Figure 2 Mesh Model

Table 1 the boundary Condition for Airfoil [17, 1]

Boundary Condition	Value
Total Temperature/K	311
Mach number	0.18
Reynolds Number	$3x10^6$
Mach Number	0.6-0.86
Angle of Attack	-16 to +16
Density	Ideal Gas
Cp	1006.43
Thermal Conductivity	0.0242
Viscosity	1.7894e-05
Molecular Weight =	28.966

V. RESULT AND DISCUSSION

The governing equations of the problem were solved, numerically, using a Element method, and finite Volume method (FVM) used in order to calculate the Aerodynamic characteristics of a Airfoil NACA0012. As a result of a grid independence study, a grid size of 10^6 was found to model accurately the aerodynamic performance characteristics are described in the corresponding results.

The accuracy of the computational model was verified by comparing results from the present study with those obtained by Harris [1], Tapan [17], [15] Experimental, Analytical and FVM results.

ISSN 2348 – 7968

Table 2 Validation of Coefficient of Drag respect to Coefficient of Lift for NACA 0012 Airfoil

S.No		1	2	3
Mach Number	M	0.6	0.779	0.82
Reynolds Number	Re	$3x10^6$	$3x10^7$	$3x10^8$
Angle of Attack	α	-0.14	-0.14	-0.14
Computed Ref.[17]	C_L	-0.0161	-0.00989	-0.0406
	C_D	0.0022	0.0057	0.0238
Experimental Ref.[1, 17]	C_L	-0.016	-0.013	-
	C_D	0.006	0.007	-
Present (ANSYS)	C_L	-0.01613	-0.0102	-0.03985
	C_D	0.00212	0.0061	0.0227

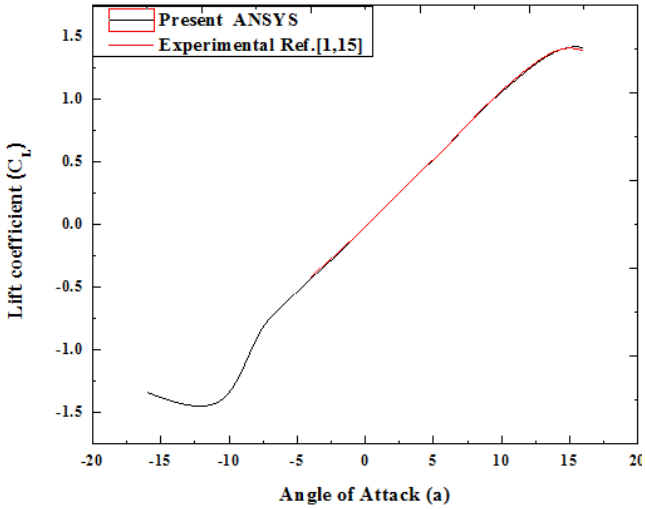

Figure 3 Validation of Lift coefficients with respect to Angle Of Attack

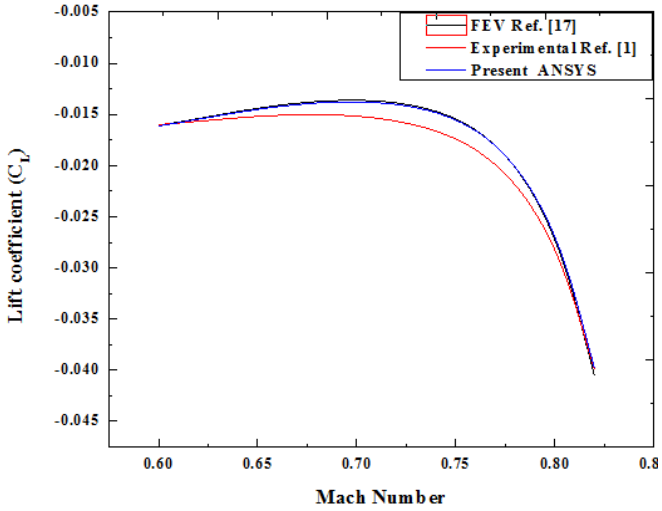

Figure 4 Validation of variation of Lift coefficient with respect to various Mach number

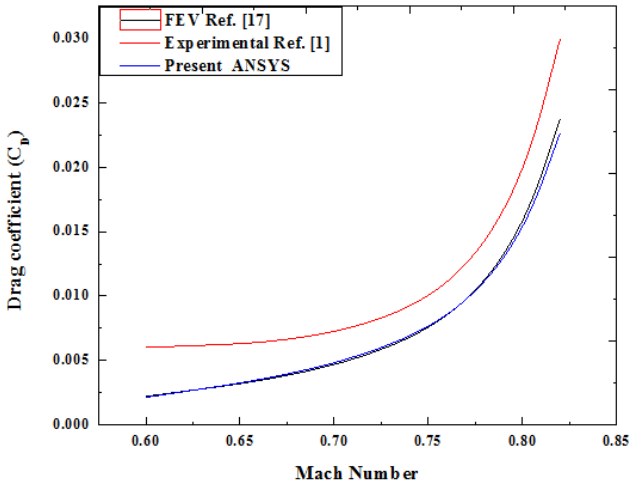

Figure 5 Validation of variation of Drag coefficient with respect to various Mach number

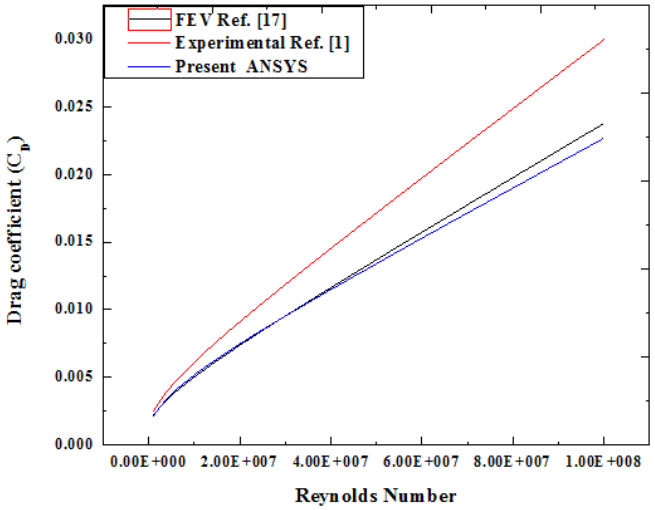

Figure 6 Validation of variation of Drag coefficient with respect to Reynolds Number

ISSN 2348 – 7968

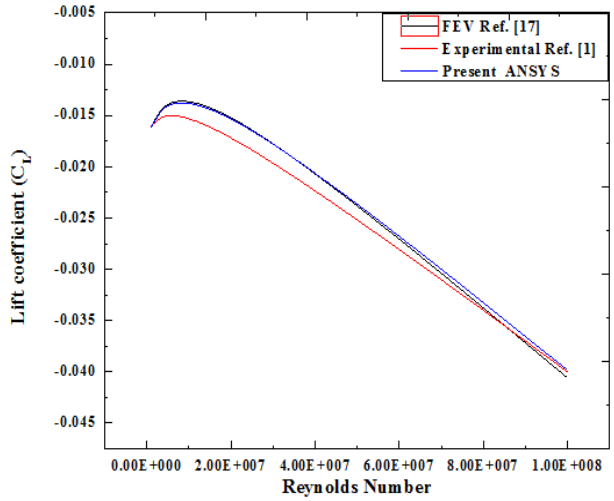

Figure 7 Validation of variation of Lift coefficient with respect to Reynolds Number

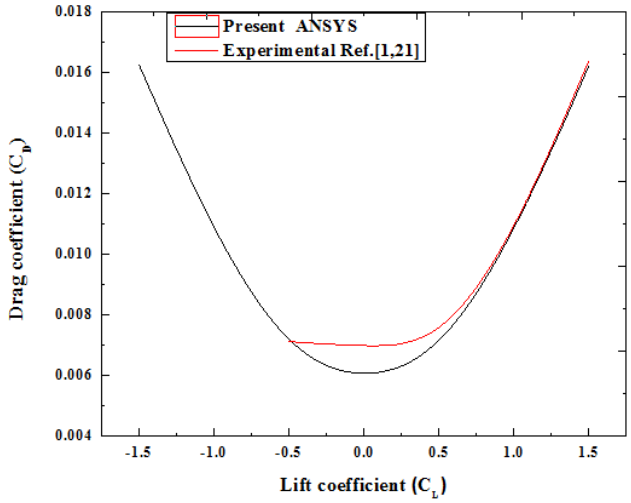

Figure 8 Validation of Coefficient of Drag with respect to Coefficient of Lift

In figure 3-8, shows the validation of FVM result obtained from the ANSYS tool. It has been seen that the obtained result of Airfoil with diffent boundary condition shows good agreement with the analalytical, Experimental and FVM of available literature.

The small variation is results is due to variation in grid sizing, operating condition, geometrical parameters, etc. but the obtained result shows the same trend so that the results are suitably verified.

Figure 9-16, shows the contour plot of an airfoil which illustrates the flow pattern across the airfoil. On the basis of this aerodynamic characteristics various graphs has been ploted and disscued there significance in airfoil performance has been stated.

It has observed that on increasing angle of attack the lift coeffiecnt lineraly increases and starts converging at $+16^0$ angle of attack, similarly in taking negative angle of attack the trend is symmetrical and converges at -16^0 angle of attack. Moreover, at +16° angle of attack Static pressure at the top surface increases and ultimately reduces lift and increases drag this phenomenon is referred as stalling.

On incresing mach no. the lift coefficient starts decline as the drag coefficient increases. As the Mach no. increases, shock waves emerge in the flow field, getting stronger as the speed increases. The shock waves lead to a swift increase in drag, both due to the emergence of wave drag, and also because the pressure rise through a shock wave thickens the boundary layer, leading to increased viscous drag. Thus cruise speed is limited by the rapid drag rise. The developed shock wave leads to dynamic instablity and it is illustrated by effective prandtl number.

At leading edge the static and dynamic pressure is minumum at the top wall surface. Which leads to increases velocity magnitude and maxminum at bottom wall surface, depending on mach no. and angle of attack in transonic flow. Therefore the top wall or upper surface is referred as pressure side and the bottom wall or lower surface referred as suction side. The flow variation has also been seen on increasing reynolds number the drag coefficient increases and lift coefficient dereases.

The stability of airfoil crucially depends upon the pitching moment of an airfoil. On increasing angle of attack pitching moment decreases. So therefore proper balance should be maintain in such a way that drag can be delayed and adequate lift can be achived without being stalled.

Since at high angle of attack flow separation takes place and develop viscous region which leads to increases in drag coeffiecnt. However the drag coefficient has two elements friction due to the shear-stress at the wall of airfoil and pressure resistance due to visous region in outer flow stream lines.

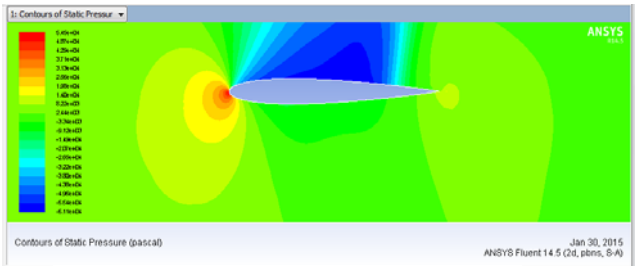

Figure 9 Contour plot of Static Pressure around Airfoil

ISSN 2348 – 7968

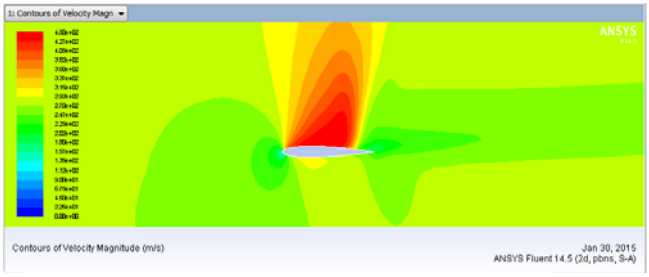

Figure 10 Contour plot of Velocity magnitude around Airfoil

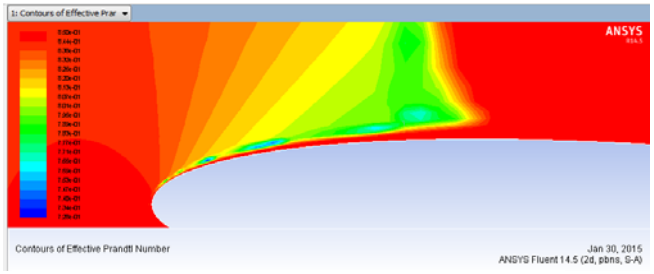

Figure 11 Contour plot (Magnified) of Effective Prandtl number over leading edge of Airfoil

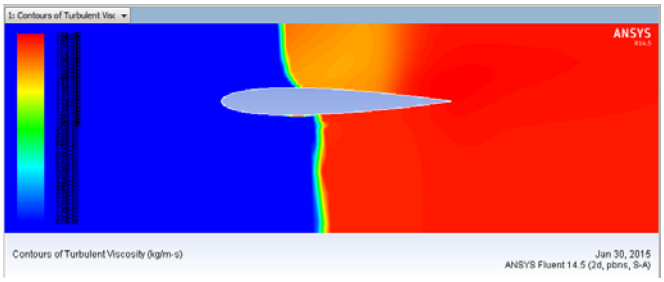

Figure 12 Contour plot of turbulent viscosity over Wall surface of Airfoil

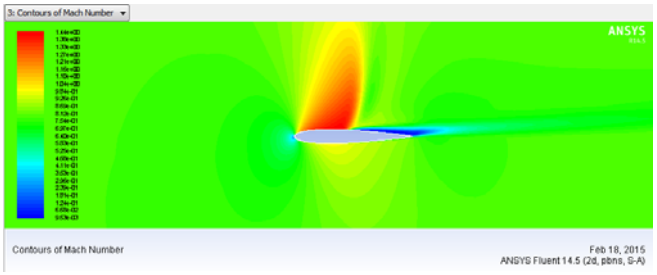

Figure 13 Contour plot of Mach number over around Airfoil

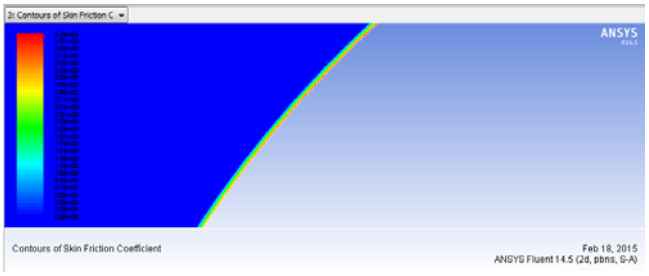

Figure 14 Contour plot of Skin Friction coefficient over Wall surface of Airfoil

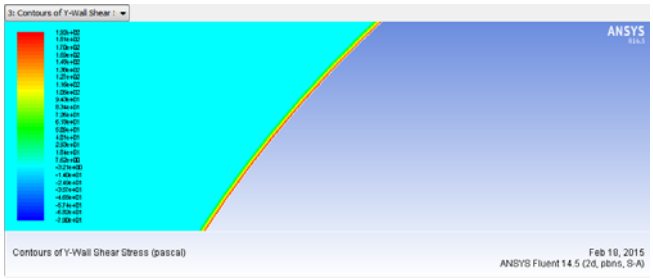

Figure 15 Contour plot of wall shear stress over Y-Wall surface of Airfoil

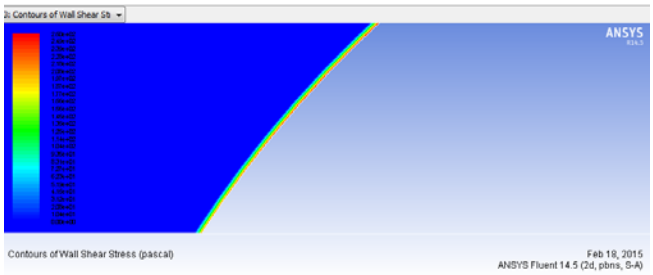

Figure 16 Contour plot of wall shear stress over Wall surface of Airfoil

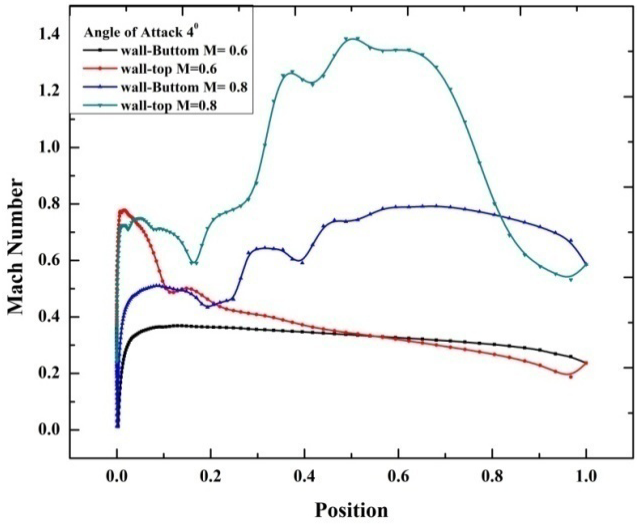

Figure 17 Variation of Mach no. on Aerofoil surface at Angle of Attack 4^0

Figure 17 and 18, shows the Variation of Mach no. on Aerofoil surface at Angle of Attack 4^0 and 6^0. On increasing mach no. the mach no over the airfoil surface first increases and then starts decreases gradually.

But on in presence of varying angle of attack the variation in mach no. throughout the airfoil surface abrupt change in mach no has been seen particularly over the top surface at Mach no. 0.8 at mid of the airfoil maximum mach no. is seen.

ISSN 2348 – 7968

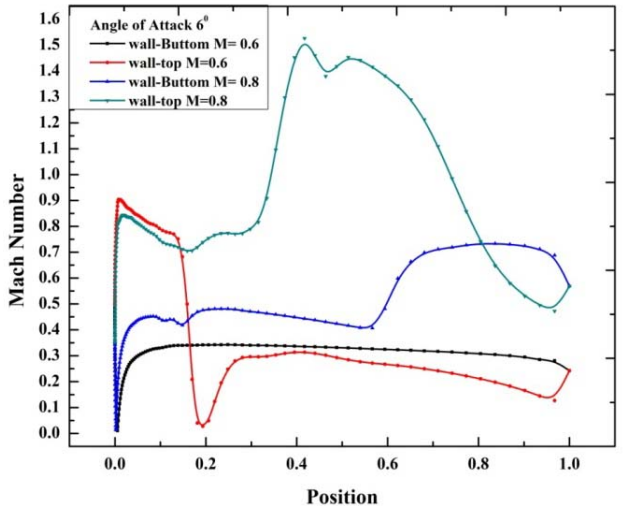

Figure 18 Variation of Mach no. on Aerofoil surface at Angle of Attack 6^0

This means that more lift has been attain. On comparing the surfaces at top surface the variation is more significant where as in bottom surface gradual decline has been seen from leading edge to the tailing edge.

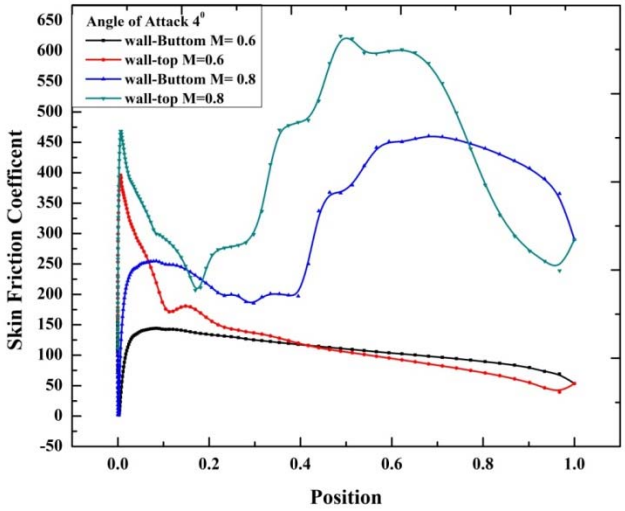

Figure 19 Variation of Skin Friction Coefficient on Aerofoil surface at Angle of Attack 4^0

The effect of Skin Friction Coefficient on Aerofoil surface at Angle of Attack 4^0 and 6^0 illustrated in figure 19 and 20. It has observed that on increasing angle of attack and mach no. the lift coefficient and drag coefficient increases correspondingly.

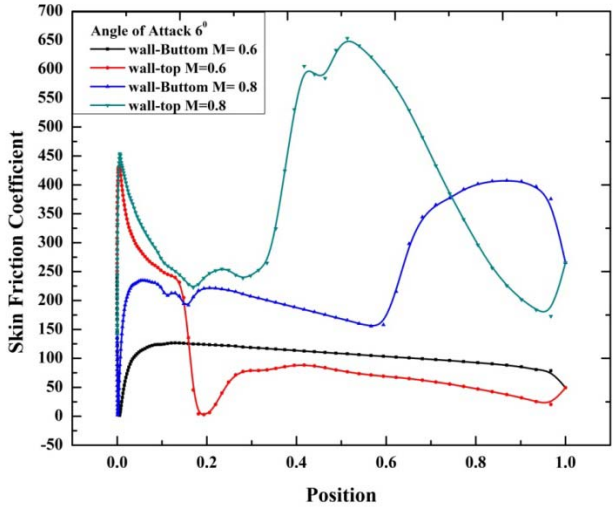

Figure 20 Variation of Skin Friction Coefficient on Aerofoil surface at Angle of Attack 6^0

Due to increase in drag skin friction coefficient increases as the air strikes the airfoil creates a drag force due to skin friction. However pressure drag have also been created due to abrupt change in airfoil surface therefore swept airfoil are recommended to overcome such effect and attain desired lift without been stalled.

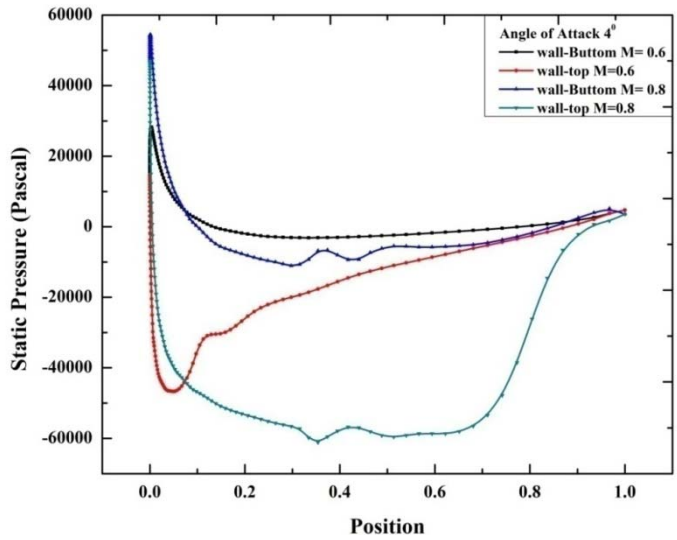

Figure 21 Variation of Static Pressure around the Aerofoil surface at Angle of Attack 4^0

Figure 21 and 22, shows the variation of Static Pressure on Aerofoil surface at Angle of Attack 4^0 and 6^0. On increasing angle of attack and Mach number emerges adverse pressure gradient which leads to flow separation. The effect is more remarkable at the leading edge of the airfoil. At the top wall or upper surface of the airfoil the influence of angle of attack has been seen for mach no. 0.6.

ISSN 2348 – 7968

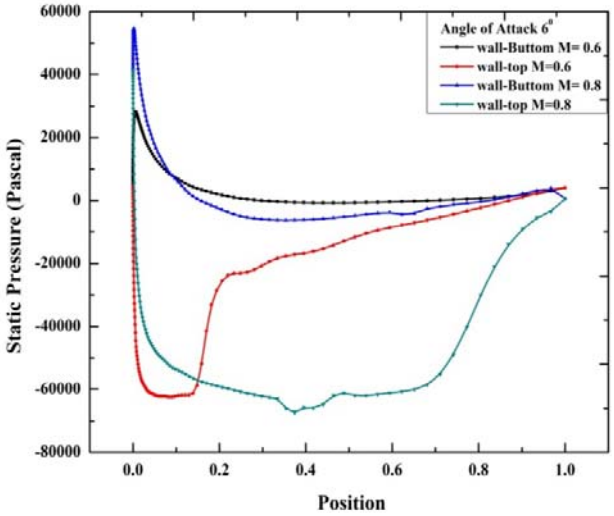

Figure 22 Variation of Static Pressure around the Aerofoil surface at Angle of Attack 6^0

The static pressure at bottom wall or lower surface first increases at the leading edge and start's decreases till it reaches the tailing edge of the airfoil. It can also be revealed that at the upper surface or top wall of airfoil, static pressure is minimum, whereas at bottom wall or lower surface static pressure is higher.

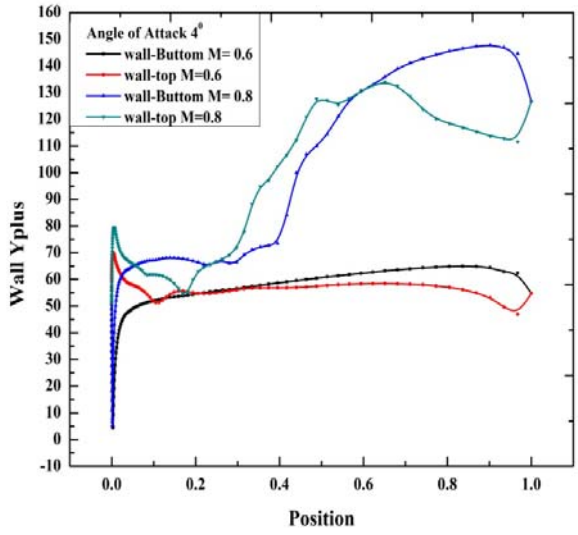

Figure 23 Variation of turbulence in Wall Y plus at Angle of Attack 4^0

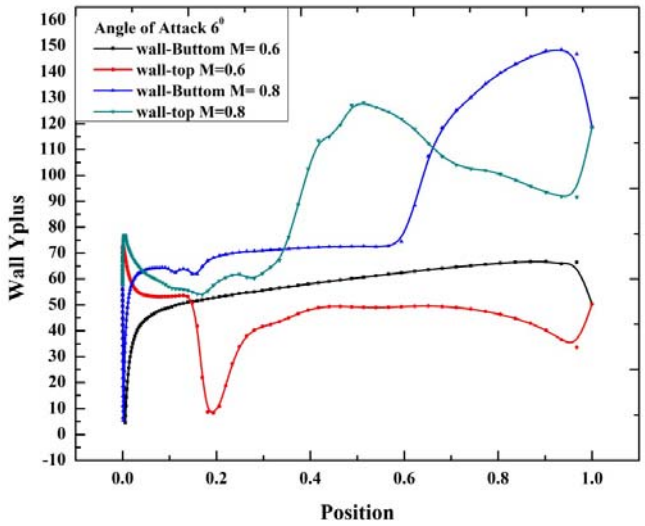

Figure 24 Variation of turbulence in Wall Y plus at Angle of Attack 6^0

The effect of turbulence is illustrated in figure 23 and 24, with the variation of angle of attack and Mach number. It has been observed that on increasing angle of attack the shock wave occurs which creates turbulence. The effect is more noteworthy in case of increasing mach no.
From it can be conclude that on increasing mach no. turbulence develop around the airfoil.

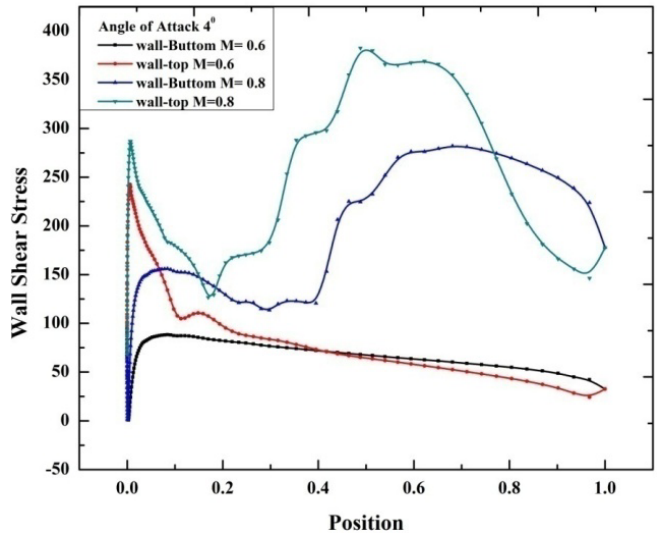

Figure 25 Variation of Wall Shear Stress on Aerofoil surface at Angle of Attack 4^0

Figure 25 and 26, shows the variation Wall Shear Stress on Aerofoil surface at Angle of Attack 4^0 and 6^0. On increasing angle of attack leads to flow separation and develop viscous region which decrease lift coefficient due to stalling.

ISSN 2348 – 7968

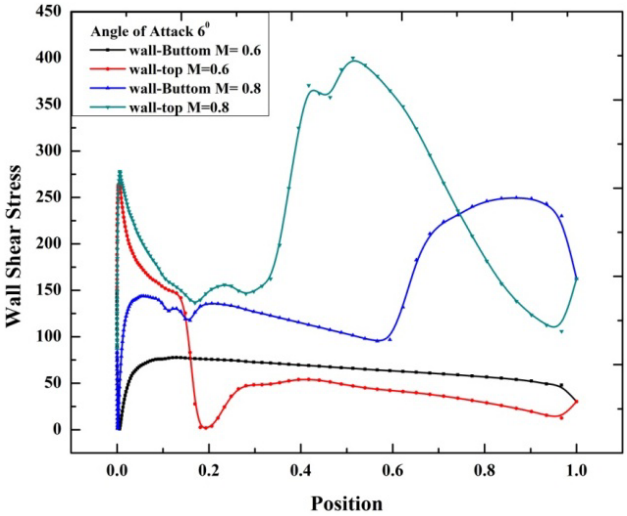

Figure 26 Variation of Wall Shear Stress on Aerofoil surface at Angle of Attack 6^0

Drag force involve two components i.e. friction due to shear stress at wall and pressure resistance which is originated by displacement imposed by viscous region to the outer flow stream-lines. Even on increasing mach no. the effect of wall shear stress is more significant at leading edge and the mid of the airfoil. Therefore in order to overcome from such as effect swept airfoil should be used.

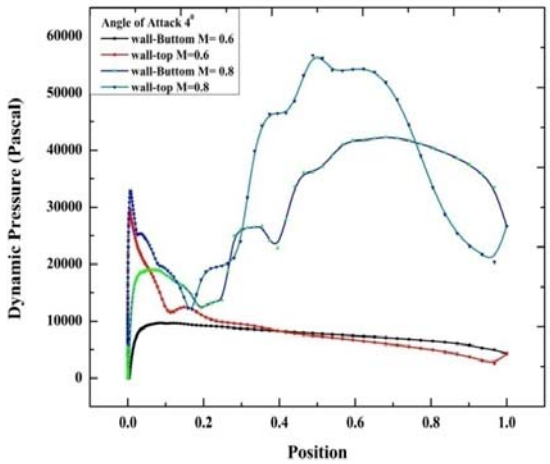

Figure 27 Variation of Dynamic Pressure on Aerofoil surface at Angle of Attack 4^0

In figure 27 and 28, shows the Variation of Dynamic Pressure on Aerofoil surface at Angle of Attack 4^0 and 6^0. The behavior of airfoil is conveniently measured in multiples of the dynamic pressure at pressure and suction side. The dynamic pressure is property of free stream that can be measure far from the wings or airfoil. It has observed that on increasing angle of attack the dynamic pressure of top wall surface at the leading edge till 0.2 increases and then starts decreases throughout the surface or airfoil.

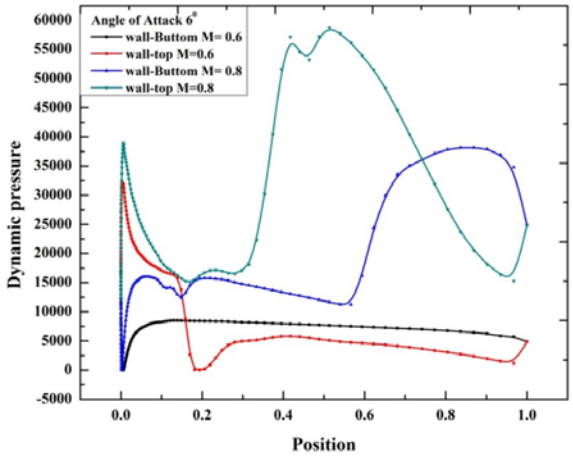

Figure 28 Variation of Dynamic Pressure on Aerofoil surface at Angle of Attack 6^0

On increasing mach no. shock wave develops and affect the dynamic pressure at the top surface at mid of the airfoil.

It can also be revealed that on increasing angle of attack and mach no. the dynamic pressure extensively affected and for remarkable at the top surface of airfoil.

VI. CONCLUSIONS

- On increasing angle of attack lift coefficient significantly increases but there is limitation of increasing angle of attack i.e. the angle of attack starts converging after $+16^0$. At angles of attack greater than that which produces the greatest amount of lift, the airfoil is said to be stalled. This occurs at 16° angle of attack. The increase in static pressure on the upper surface dramatically reduces lift and increases drag.
- The effect of mach no. is vice versa in lift coefficient and Drag coefficient.
- Effective Prandtl Number signifies the turbulent characteristics within zones of shock wave produce around the airfoil which causes dynamic instability.
- As the Mach number increases, shock waves appear in the flow field, getting stronger as the speed increases. The shock waves lead to a rapid increase in drag, both due to the emergence of wave drag, and also because the pressure rise through a shock wave thickens the boundary layer, leading to increased viscous drag. Thus cruise speed is limited by the rapid drag rise.
- Swept wings have to be used in order to reduce drag at high mach no.
- Pitching moment change with Mach

number (Mach tuck), and Mach induced changes in control effectiveness.

- Is possible to design an airfoil to have a shock-free recompression, this situation is usually possible for only a single combination of Mach number and lift coefficient
- Most foil shapes require a positive angle of attack to generate lift, but cambered airfoils can generate lift at zero angle of attack. This "turning" of the air in the vicinity of the airfoil creates curved streamlines which results in lower pressure on one side and higher pressure on the other. This pressure difference is accompanied by a velocity difference, via Bernoulli's principle, so the resulting flow field about the airfoil has a higher average velocity on the upper surface than on the lower surface.

REFERENCES

[1] Harris CD. "Two-dimensional aerodynamic characteristics of the NACA0012 airfoil in the Langley 8-foot transonic pressure tunnel". NASA TM-81927; 1981

[2] Peter M. Goorjian, Guru P. Guruswamy, "Transonic unsteady aerodynamic and aeroelastic calculations about airfoils and wings",Computers & Structures, Volume 30, Issue 4, 1988, Pages 929-936

[3] Ünver Kaynak, Jolens Flores, "Advances in the computation of transonic separated flows over finite wings",Computers & Fluids, Volume 17, Issue 2, 1989, Pages 313-332

[4] Aparajit J Mahajan, Earl H Dowell, Donald B Bliss, "Eigenvalue calculation procedure for an Euler/Navier-Stokes solver with application to flows over airfoils",Journal of Computational Physics, Volume 97, Issue 2, December 1991, Pages 398-413

[5] S. Yang, I. Lee, "Aeroelastic analysis for flap of airfoil in transonic flow", Computers & Structures, Volume 61, Issue 3, November 1996, Pages 421-430

[6] Angelo Iollo, Manuel D. Salas,"Optimum transonic airfoils based on the Euler equations", Computers & Fluids, Volume 28, Issues 4–5, May–June 1999, Pages 653-674

[7] Fue-Sang Lien, Georgi Kalitzin, "Computations of transonic flow with the v2–f turbulence model",International Journal of Heat and Fluid Flow, Volume 22, Issue 1, February 2001, Pages 53-61

[8] J. Fořt, J. Fürst, K. Kozel, A. Jirásek, M. Kladrubský, "Numerical Solution of 2D and 3D Transonic Flows Over an Airfoil and a Wing", Fluid Mechanics and its Applications Volume 73, 2003, pp 211-216

[9] Yongsheng Lian, Jonas Steen, Marcus Trygg-Wilander, Wei Shyy, "Low Reynolds number turbulent flows around a dynamically shaped airfoil", Computers & Fluids, Volume 32, Issue 3, March 2003, Pages 287-303

[10] Jiang-feng WANG, Yi-zhao WU, "Hierarchical Evolutionary Algorithms and Its Application in Transonic Airfoil Optimization in Aerodynamics", Chinese Journal of Aeronautics, Volume 16, Issue 1, February 2003, Pages 1-6

[11] Jose L. Vadillo, Ramesh K. Agarwal, Ahmed A. Hassan, "Active Control of Shock/Boundary Layer Interaction in Transonic Flow Over Airfoils", Computational Fluid Dynamics 2004 2006, pp 361-366

[12] P. Cinnella, P.M. Congedo, "Optimal airfoil shapes for viscous transonic flows of Bethe–Zel'dovich–Thompson fluids",Computers & Fluids, Volume 37, Issue 3, March 2008, Pages 250-264

[13] C. Wollblad, L. Davidson, L.-E. Eriksson, "Investigation of large scale shock movement in transonic flow", International Journal of Heat and Fluid Flow, Volume 31, Issue 4, August 2010, Pages 528-535

[14] Rémi Bourguet, Marianna Braza, Alain Dervieux, "Reduced-order modeling of transonic flows around an airfoil submitted to small deformations", Journal of Computational Physics, Volume 230, Issue 1, 1 January 2011, Pages 159-184

[15] 2D NACA 0012 Airfoil Validation, Langley Research Center Turbulence Modeling Resource, http://turbmodels.larc.nasa.gov/naca0012_val.html 1/8

[16] Alexander Kuzmin, "Non-unique transonic flows over airfoils", Review Article Computers & Fluids, Volume 63, 30 June 2012, Pages 1-8

[17] Tapan K. Sengupta, Ashish Bhole, N.A. Sreejith, "Direct numerical simulation of 2D transonic flows around airfoils", Computers & Fluids, Volume 88, 15 December 2013, Pages 19-37

[18] Joachim Klinner, Alexander Hergt, Christian Willert, "Experimental investigation of the transonic flow around the leading edge of an eroded fan airfoil", Experiments in Fluids, August 2014, 55:1800, Date: 24 Aug 2014

[19] R. Mukesh K. Lingadurai, U. Selvakumar, "Airfoil shape optimization using non-traditional optimization technique and its validation", Journal of King Saud University – Engineering Sciences (2014) 26, 191–197

[20] B. Yang, Q. Xu, L. He, L. H. Zhao, Ch. G. Gu and P. Ren, "A Novel Global Optimization Algorithm and Its Application to Airfoil Optimization",J. Turbomach. 137(4), 041011 (Apr 01, 2015)